

Article

The Influence of Common Monovalent and Divalent Chlorides on Chalcopyrite Flotation

Yubiao Li ^{1,2,*} , Wanqing Li ¹, Qing Xiao ², Nan He ¹, Zijie Ren ¹, Clement Lartey ¹ and Andrea R. Gerson ³

¹ School of Resources and Environmental Engineering, Wuhan University of Technology, Wuhan 430070, China; wanqing280@163.com (W.L.); 15071223754@163.com (N.H.); rzj424711087@163.com (Z.R.); cle.lartey@yahoo.com (C.L.)

² School of Natural and Built Environments, University of South Australia, Mawson Lakes, SA 5095, Australia; qing.xiao@mymail.unisa.edu.au

³ Blue Minerals Consultancy, Middleton, SA 5213, Australia; andrea.gerson@bigpond.com

* Correspondence: Yubiao.Li@whut.edu.cn

Received: 2 June 2017; Accepted: 26 June 2017; Published: 1 July 2017

Abstract: Much attention has been paid to the flotation of chalcopyrite using saline seawater. However, the influence of salt ions on mineral flotation is complex, and different salts may play various roles—either beneficial or detrimental. This study investigated the effects of common chlorides (Cl^-) of Na^+ , K^+ , Mg^{2+} , and Ca^{2+} in seawater on chalcopyrite floatability. The presence of Na^+ , K^+ , and Ca^{2+} resulted in greater chalcopyrite recovery, with this effect being more pronounced for the monovalent cations. In contrast, the addition of Mg^{2+} resulted in decreased chalcopyrite flotation efficiency. Contact angle measurements showed that the presence of monovalent cations increased the hydrophobicity of the chalcopyrite surface, while the presence of divalent cations reduced its hydrophobicity, depending on the concentration. Zeta potential, pulp species, and X-ray photoelectron spectroscopy (XPS) cross-confirmed the precipitation of $\text{Mg}(\text{OH})_2$ on the chalcopyrite surface when Mg concentration was 10^{-2} M and pulp pH was 10.

Keywords: chalcopyrite; flotation; chlorides; zeta potential; contact angle

1. Introduction

Chalcopyrite (CuFeS_2) comprises nearly 70% of the Earth's copper resources, and is the most important and abundant cupriferous mineral [1,2]. Chalcopyrite is typically processed pyrometallurgically subsequent to its separation from gangue minerals by flotation which is a water-intensive process based on the different natural or induced surface properties of the valuable and gangue minerals [3–5]. However, due to the scarcity of fresh water and stringent environmental regulations regarding the quality of discharged water, many flotation plants have to use recycled water or sea water—both of which contain a high concentration of electrolytes [6–8]. For instance, Las Luces—a copper–molybdenum plant in Chile—utilizes seawater mixed with tailings dam water for ore grinding and flotation [9]. Batu Hijau Concentrator in America (Newmont, operating from 2000) uses sea water to process gold-rich porphyry copper ore [10]. Inevitably, the application of highly saline slurries results in challenging flotation process control issues, frequently associated with the maintenance of grade and recovery while minimizing the dosage of reagents.

The presence of salt ions in the flotation slurry increases the complexity of pulp aqueous environment by affecting the structure of the water surrounding mineral particles [11–14], particle surface properties [15–17], and bubble properties [18–21]—all of which influence the mineral–bubble interaction and flotation efficiency [6].

In the flotation process, frothers are normally employed to inhibit bubble coalescence, stabilize the froth by dispersing air [22], and provide adequate frothing characteristics [23,24]. The presence of inorganic salts leads to more complex bubble coalescence, as inorganic ions—similar to frothers—can stabilize foams against coalescence and reduce bubble size [19,25]. The effects of salts on both floatability and frothability have been examined for copper ores [3,19,21,22,26–30]. However, the effects of frothing characteristics of specific chloride salts on chalcopyrite flotation remain unclear.

Suyantara et al. [27] found that the hydrophobic chalcopyrite surfaces became hydrophilic in 10^{-2} M MgCl_2 solution at high pH due to the precipitation of $\text{Mg}(\text{OH})_2$ onto the mineral surfaces. Hirajima et al. [3] reported that high concentrations of divalent cations (i.e., Ca^{2+} and Mg^{2+}) reduced chalcopyrite floatability at pH greater than 9, owing to the surface adsorption of $\text{Mg}(\text{OH})_2$ and CaCO_3 precipitates, thereby reducing surface hydrophobicity. In addition, Ramos et al. [22] investigated copper ores flotation in sea water (major cations include 0.6 M Na^+ , 1300 ppm Mg^{2+} , and 400 ppm Ca^{2+}) and observed that chalcopyrite floatability was slightly reduced in sea water as compared to fresh water under alkaline conditions. However, the effects of each cation at different concentrations were not examined. Copper flotation recoveries using distilled water and seawater were found to be similar in lab-scale studies by Aral et al. [30] and Corin et al. [21], but deteriorated at greater ionic strengths. Jeldres et al. [29] studied the impact of seawater ions on the flotation of copper-molybdenum sulfides. By adding $\text{CaO-Na}_2\text{CO}_3$ mixtures, a significant portion of the divalent ions— Ca^{2+} and Mg^{2+} —was removed and the flotation showed rapid increase in both chalcopyrite and molybdenite recovery.

In contrast to the examination of divalent cations, the specific effects of monovalent cations on chalcopyrite floatability have not attracted much attention. In order to utilize seawater or high salt concentration solutions containing both monovalent (e.g., Na^+ , K^+) and divalent (e.g., Ca^{2+} , Mg^{2+}) cations, it is important and necessary to understand the effects of these cations on chalcopyrite floatability. In the present study, we focused on the effects on chalcopyrite flotation of four seawater-containing chloride salts (Na^+ , K^+ , Mg^{2+} , and Ca^{2+}) in a laboratory-scale mechanical flotation cell. The zeta potential, contact angle, pulp species of these salt ions on chalcopyrite, as well as the surface species were studied to further reveal changes in the chalcopyrite flotation processes in the presence of differing cations.

2. Materials and Methods

2.1. Materials

Chalcopyrite samples used in this study were purchased from GEO discoveries, Australia. Prior to wet sieving, the chalcopyrite was crushed and ball milled. The clinging fines were removed from the resulting samples via sonication. The samples were then dried in a vacuum oven at 30 °C for 24 h. Subsequently, the dried powder samples were transferred into plastic tubes which were sealed after being filled with N_2 gas to minimize surface oxidation by air. All the samples were stored in a freezer prior to flotation and related measurements. The X-ray powder diffraction indicated that the majority of the sample was well-crystallized chalcopyrite.

Analytical-grade collector (sodium butyl xanthate) was used, and technical grade terpenic oil was used as the frother. NaOH and HCl were used for solution pH adjustment. Millipore® (Billerica, MA, USA) ultrapure water with a resistivity of 18.2 $\text{M}\Omega\cdot\text{cm}$ was employed in all measurements except flotation experiments using distilled water.

2.2. Flotation Experiments

All chalcopyrite flotation tests were conducted using a hanging trough-type flotation machine (XFGII5–35g, Wuhan Exploration Machinery Factory, Wuhan, China) at 1200 rpm with an airflow rate of 80 $\text{mL}\cdot\text{min}^{-1}$. Chalcopyrite powder (2 g) with a particle size of 38–75 μm was suspended in 25 mL of solution containing chloride salts (NaCl , KCl , CaCl_2 , and MgCl_2) at various concentrations. The pulp pH was adjusted to 10 within 3 min using NaOH, followed by the addition of butyl xanthate

collector within 1 min. Thereafter, terpenic oil was added and mixed for 1 min prior to froth collection at 1, 3, 5, and 8 min. Both the floated and unrecovered fractions were collected and air dried at 70 °C for 2 h prior to weighing.

2.3. Zeta Potential Measurements

Chalcopyrite samples (0.5 g, $-38\ \mu\text{m}$) were placed into 50 mL NaCl, KCl, CaCl_2 , and MgCl_2 solutions at various concentrations. During stirring for 3 min, the solution pH was adjusted to designed value ranging from 2 to 10 using NaOH and HCl. The agitated suspension was then sampled for zeta potential measurements (Zetasizer Nano-zs90, Malvern Co., Ltd., Malvern, UK). The results presented were the average of three independent measurements, with a typical variation of ± 5 mV.

2.4. Contact Angle Measurements

Chalcopyrite slab samples were progressively polished using 600, 1000, and 5000 mesh metallographic abrasive papers, providing a flat surface. Ethanol was applied to clean the surface, which was subsequently carefully dried using filter papers. Prior to contact angle measurements, each chalcopyrite slab was treated for 3 min in a solution containing the same salt concentrations as for flotation. This was then followed by butyl xanthate addition into the solution to react with the slab sample for 0, 1, 3, 5, and 8 min, respectively. All the measurements were repeated at least three times, and the average values are reported herein. The sessile drop technique (JC2000C1, Shanghai Zhongchen Digital Technology Company, Shanghai, China) was applied to measure contact angles of chalcopyrite surface. After a drop (0.25 μL) of Millipore[®] ultrapure water being placed onto the chalcopyrite slab surface through a microliter syringe, the profile of contact angle was imaged within 30 s and processed using JC2000D software.

2.5. X-ray Photoelectron Spectroscopy (XPS) Analysis

The X-ray photoelectron spectroscopy was conducted using ESCALAB 250Xi (Thermo Fisher Scientific Inc., Waltham, MA, USA) equipped with an Al $K\alpha$ monochromatic X-ray source. The survey spectra were collected from 1350 to 0 eV with a pass energy of 30 eV and a step size of 0.1 eV. The spectra and surface atomic ratios were obtained and calculated through Thermo Avantage software using Shirley method [31] for background corrections. The binding energy of C 1s at 284.8 eV was used as an internal standard for calibration [32].

3. Results and Discussion

3.1. Effects of Reagent Dosages

Figure 1a shows the chalcopyrite recovery on addition of various amounts of terpenic oil (frother) and 30 ppm butyl xanthate (collector). The cumulative recovery of chalcopyrite increased significantly when the frother dosage was increased from 5 to 10 ppm. However, when terpenic oil was further increased to 15 ppm, the cumulative recovery did not increase significantly. However, a more significant increase was observed at a lower frother concentration of 5 ppm between 1 and 8 min flotation time, as compared to that over the same time period at 10 and 15 ppm frother. Therefore, 10 ppm was selected as the optimal frother dosage for further flotation experiment, with an approximately 80% recovery after 8 min.

Figure 1b shows the effects of collector dosage, with a frother dosage of 10 ppm. The cumulative recovery of chalcopyrite increased significantly with increasing butyl xanthate concentration from 20 to 30 ppm. However, no significant increase was observed on further collector dosage increasing to 50 ppm. Therefore, the collector dosage of 30 ppm was applied for further study.

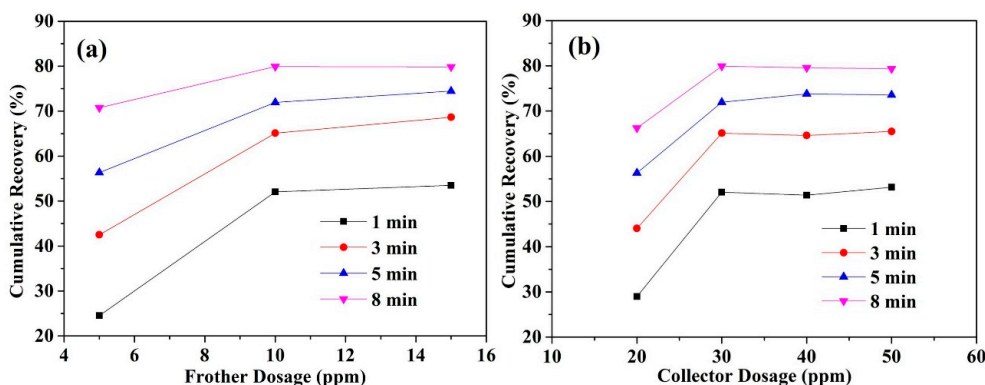


Figure 1. The effects of (a) frother and (b) collector on chalcopyrite recovery.

3.2. Effects of Salts

Figure 2 shows the effects of typical soluble chloride salts on chalcopyrite flotation. As the pulp was adjusted to pH 10 using NaOH, approximately 10^{-4} M Na^+ was added to the slurry, which was present as a background Na^+ concentration. Therefore, the effect of Na^+ was limited to the addition of 10^{-2} and 10^{-1} M to negate the Na^+ background effects. It is observed that the addition of NaCl, KCl, and CaCl_2 resulted in greater chalcopyrite recovery (Figure 2a–c). In contrast, the presence of MgCl_2 decreased chalcopyrite flotation recovery, especially at a high concentration of 10^{-2} M (Figure 2d).

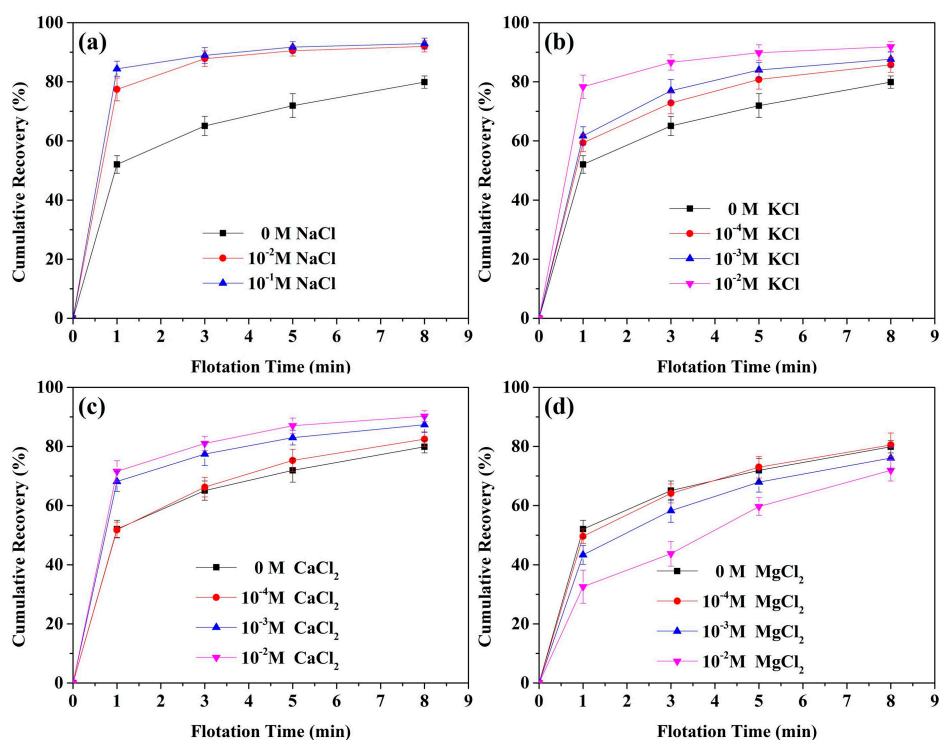


Figure 2. The effects of salts on chalcopyrite recovery: (a) NaCl; (b) KCl; (c) CaCl_2 ; and (d) MgCl_2 .

Specifically, the chalcopyrite recovery increased rapidly within the first 1 min, from 52% (0 M Na^+) to 77% and 84%, with an increase in Na^+ concentration from 10^{-2} and 10^{-1} M, respectively (Figure 2a). Three minutes later, no significant difference in chalcopyrite recovery was observed due to increased Na^+ concentration, eventually achieving an approximately 92% recovery at 8 min, but still significantly greater than that without Na^+ addition. The cumulative recovery of chalcopyrite gradually increased when KCl concentration was increased from 10^{-4} to 10^{-2} M (Figure 2b). It should be noted

that the addition of 10^{-2} M KCl had an almost equivalent effect to NaCl at the same concentration. These results indicated that the presence of monovalent cations is beneficial to chalcopyrite flotation at the concentration range examined.

Ca^{2+} addition was observed to be beneficial (Figure 2c), while Mg^{2+} was detrimental (Figure 2d) to chalcopyrite flotation. Chalcopyrite recovery was not significantly improved in the presence of 10^{-4} M Ca^{2+} solution, but apparently greater chalcopyrite recovery was obtained on increased Ca^{2+} concentration to 10^{-3} M, with a further slight increase in chalcopyrite recovery at 10^{-2} M Ca^{2+} . The recovery within the first minute in 10^{-2} M CaCl_2 solution was only 71.6% as compared to 77% in 10^{-2} M NaCl and KCl solutions, indicating that monovalent cations had a more positive effect on chalcopyrite flotation. CaCl_2 was reported to have negligible effects by Nagaraj and Farinato [33], while Hirajima et al. [3] reported the effects to be negative. Such contrasting results are likely due to the differences in pulp density and flotation reagents influencing the mineral floatability by changing the frothability of seawater solutions [22], e.g., Nagaraj and Farinato [33] used a very high pulp density (35 wt.%) with added sodium diisobutyl dithiophosphate as the collector, while Hirajima et al. [3] used a very low pulp density (0.03 wt %) using a Hallimond tube.

Although chalcopyrite recovery was not significantly reduced in the presence of 10^{-4} M Mg^{2+} , this effect increased on increasing Mg^{2+} concentration to 10^{-2} M (Figure 2d). Detrimental effects of MgCl_2 on chalcopyrite floatability at high pH has been reported by Hirajima et al. [3] and Nagaraj and Farinato [33].

3.3. Contact Angle

Figure 3 shows the contact angles for chalcopyrite surfaces treated with various salt solutions for different exposure time from 1 to 8 min. It was found that the contact angle of freshly polished chalcopyrite immersed in pH 10 solution was approximately 62° , close to the value reported by Hirajima et al. [3]. The eventual contact angle (exposure time of 8 min) of the chalcopyrite treated in solution containing either KCl or NaCl was around 90° , indicating successful adsorption of butyl xanthate onto the chalcopyrite surfaces. Specifically, the addition of these two monovalent salts had a positive effect on the adsorption of collector onto mineral surface before 3 min, which further increased the contact angle of the chalcopyrite surface, indicating that the process of collector absorption on the chalcopyrite surface was achievable during this short period. These results are in accordance with the chalcopyrite flotation (Figure 2a,b), confirming that NaCl and KCl can promote chalcopyrite floatability by increasing xanthate adsorption on chalcopyrite surface within a shorter time compared to the pulp without salts, further illustrating that NaCl and KCl were beneficial to improving chalcopyrite flotation rate, especially within 3 min. The above positive roles of cations in increasing mineral flotation recovery may be attributed to the lower stability of hydration layer on samples in solutions with higher ionic strength. Blake and Kitchener [34] reported that the stable films of hydration layer were reduced when KCl concentration was gradually increased. Laskowski [35] conducted coal flotation using inorganic salts (NaCl and KCl) and proposed that the electrical double layer around the particles was compressed, resulting in the opening of hydrophobic surface sites which may attract bubbles by hydrophobic bonding. In addition, these studies suggested that the addition of salt decreased the energy barrier in wetting film rupture by compressing the electrostatic double-layer force, which is beneficial to the mineral flotation.

Figure 3c,d showed the contact angle of chalcopyrite treated in CaCl_2 and MgCl_2 solution. It was observed that the contact angles increased slightly on the addition of 10^{-4} M CaCl_2 with a slightly negative effect on increased CaCl_2 concentration (10^{-3} – 10^{-2} M), suggesting that CaCl_2 had an insignificant impact on chalcopyrite wettability. However, Figure 3d indicated that the contact angle of chalcopyrite was greatly decreased with increasing MgCl_2 concentration, although a low concentration (10^{-4} M) had unapparent effect, indicating that the presence of MgCl_2 depressed the adsorption of collector on chalcopyrite. Increased surface wettability stabilizes the liquid layer on the surface and lengthens the induction time (i.e., the time required for bubbles to remove the intervening

liquid layer on particle surfaces and form bubble-particle attachments), resulting in poor mineral flotability [3]. Suyantara et al. [27] demonstrated that the induction time was longer on chalcopyrite and molybdenite surfaces in a 10^{-2} M MgCl_2 solution at high pH values, due to the adsorption of $\text{Mg}(\text{OH})_2$ precipitation and decreased surface hydrophobicity.

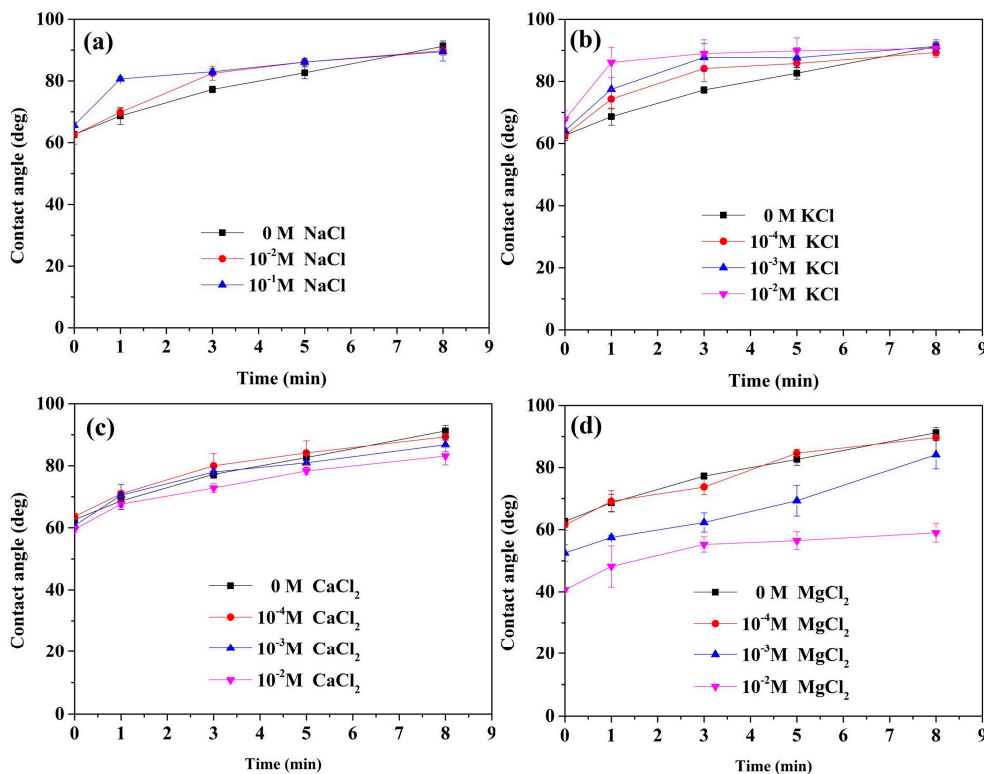


Figure 3. Contact angle of chalcopyrite surface exposed to collectors for various times in (a) NaCl; (b) KCl; (c) CaCl_2 ; and (d) MgCl_2 solution. Each measurement was finished within 30 s.

3.4. Zeta Potential

Figure 4 shows the zeta potentials of chalcopyrite in the presence of NaCl, KCl, CaCl_2 , and MgCl_2 . The overall zeta potentials were gradually decreased to more negative values with increased pH. More importantly, the zeta potential became less negative on increasing salt concentration, indicating a decrease in the electrostatic repulsion between solid surfaces at high salt concentrations. For instance, when NaCl concentration was 10^{-1} M (Figure 4a), the zeta potential was significantly increased at all pH examined. In contrast, the zeta potentials in KCl solution remained in a relatively narrow range across all pH values (Figure 4b), especially at pH 10 which was used for the flotation experiment. This indicates that KCl had no significant effect on the zeta potential of chalcopyrite.

A similar change in the zeta potential as for NaCl addition was observed in CaCl_2 solution (Figure 4c); i.e., it increased with increased CaCl_2 concentration, although no further increment was observed when CaCl_2 was in the range of 10^{-3} – 10^{-2} M, indicating that the effect of CaCl_2 on zeta potential achieved a plateau at this concentration range. Therefore, the increase in the flotability of chalcopyrite in CaCl_2 solution (Figure 2c) was mainly attributed to changed zeta potential (Figure 4c), rather than wettability (Figure 3c). In contrast to the zeta potential trends observed for other chloride salts, the zeta potentials became positive values in 10^{-3} and 10^{-2} M MgCl_2 solutions at pH 10. Therefore, the poor flotability of chalcopyrite at pH 10 in the presence of MgCl_2 was largely due to the adsorption of $\text{Mg}(\text{OH})_2$ precipitation [3], which reversed the zeta potential of the chalcopyrite surface and reduced the hydrophobicity (10^{-2} M vs. 0 M, Figure 3d). The $\text{Mg}(\text{OH})_2$ precipitation will be verified in Sections 3.5 and 3.6 through solution speciation calculation and XPS analysis.

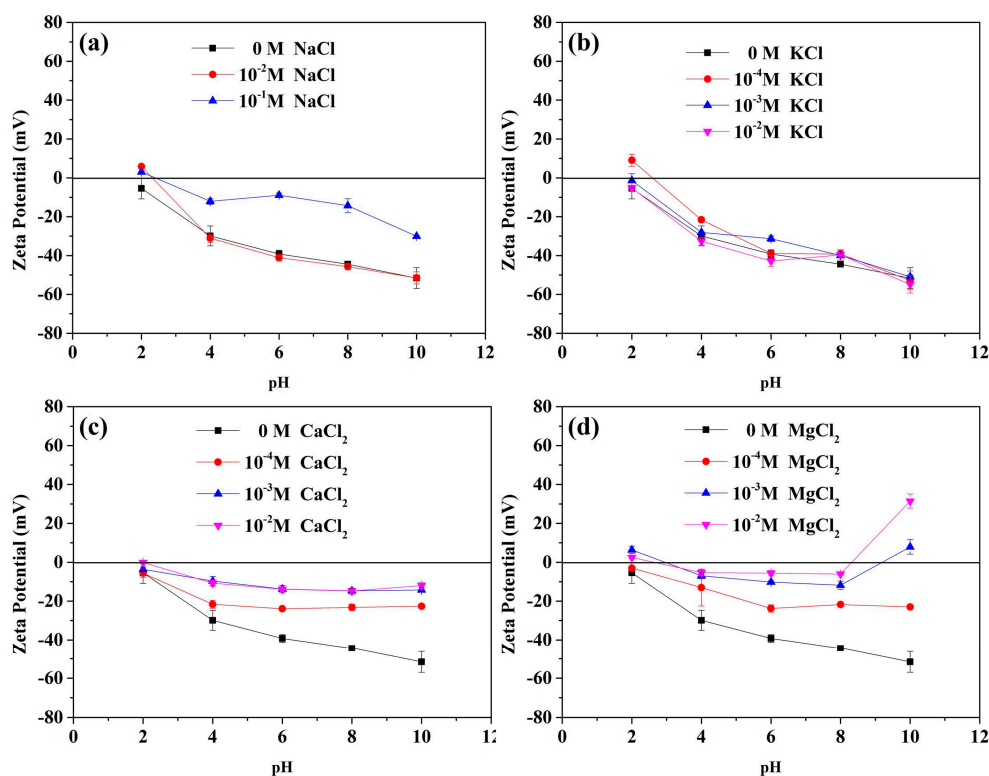


Figure 4. Zeta potential of chalcopyrite in (a) NaCl; (b) KCl; (c) CaCl₂; and (d) MgCl₂ solutions at various concentrations and pH.

3.5. Solution Species

Various chalcopyrite flotation behaviors due to the presence of different salts can be further explained by the solution species diagrams shown in Figure 5. No Ca precipitation was expected at pH below 10 when its concentration was increased from 10^{-4} to 10^{-2} M. However, the precipitation pH for Mg(OH)₂ was reduced from 10.6 to 9.6 when Mg²⁺ concentration was increased from 10^{-4} to 10^{-2} M, respectively, similar to that observed by Li and Somasundaran [36]. This further confirms the precipitation of Mg(OH)₂ in the flotation system when the pH of the pulp in the presence of 10^{-2} M Mg²⁺ was controlled at 10. Ramos et al. [22] reported that the charge of the bubble should be considered during flotation process, especially when cationic hydroxyl complexes were formed in the pulp. It was reported that the magnesium hydroxyl complexes and hydroxide formed were affinity approaching the liquid/gas interface, resulting in positively charged bubbles [36]. Similarly, magnesium hydroxyl complexes and hydroxide precipitated on chalcopyrite surface results in a positively-charged mineral surface, strongly influencing the flotation process, consistent with the observation shown in Figure 4d.

Therefore, the decrease in chalcopyrite flotability may be attributed to the increase of mineral surface wettability due to precipitation occurring at high Mg²⁺ concentrations and pH. In other words, the presence of a certain amount of Mg²⁺ is detrimental to chalcopyrite flotation, while the beneficial pH for chalcopyrite flotation should be controlled lower than the critical value when Mg²⁺ is present. This is also consistent with the flotation results shown in Figure 2 and the contact angle shown in Figure 3, where 10^{-4} Mg²⁺ had a slight influence while 10^{-2} M Mg²⁺ significantly affected chalcopyrite recovery and contact angle at pH 10.

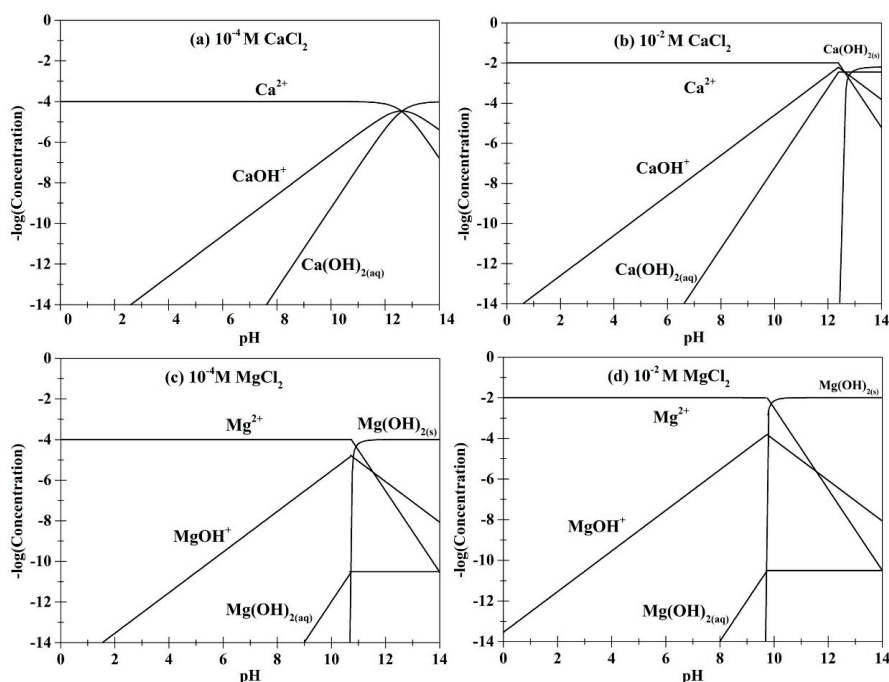


Figure 5. Ca and Mg species at 10^{-2} and 10^{-4} M.

3.6. XPS Measurements

The chalcopyrite samples floated from the pulp in the presence of 10^{-4} and 10^{-2} M Mg^{2+} were collected and dried for XPS analysis. Figure 6 shows the survey of these two chalcopyrite surfaces.

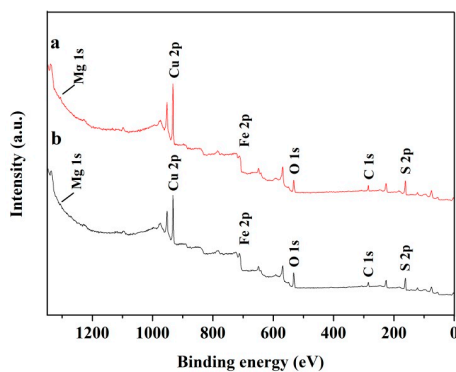


Figure 6. X-ray photoelectron spectroscopy (XPS) survey spectra of chalcopyrite surface in the presence of (a) 10^{-2} M and (b) 10^{-4} M Mg^{2+} .

Table 1 shows that the elemental composition of the chalcopyrite surfaces. It is obvious that the Mg on the chalcopyrite surface floated with 10^{-2} M $MgCl_2$ was 2 at %, while less than 1 at % Mg was observed on the chalcopyrite surface floated with 10^{-4} M $MgCl_2$ during the flotation process, further confirming the precipitation of $Mg(OH)_2$ in the presence of 10^{-2} M $MgCl_2$.

Table 1. Elemental composition of floated chalcopyrite surface.

MgCl ₂ Concentration (M)	at %				
	Cu 2p	S 2p	Fe 2p	O 1s	Mg 1s
10^{-2}	24	38	6	30	2
10^{-4}	21	35	8	36	<1

4. Conclusions

The effects of four salts—NaCl, KCl, CaCl₂ and MgCl₂—at pH 10 on chalcopyrite flotability were investigated. Both NaCl and KCl were found to be beneficial to the recovery of chalcopyrite, suggesting that monovalent cations improve the flotation response of chalcopyrite, possibly due to lower energy barrier and stability of hydration layer on chalcopyrite surface through compressing the electrostatic double-layer force.

In contrast, the addition of the divalent salts CaCl₂ and MgCl₂ showed only a slightly beneficial effect and a negative effect, respectively. The effects of CaCl₂ may be due to the decreased electrostatic repulsion between solid surfaces at pH 10. The depression caused by MgCl₂ at high concentrations was mainly due to the adsorption of Mg(OH)₂ precipitates on the chalcopyrite surfaces, reducing chalcopyrite surface hydrophobicity.

Acknowledgments: This work was financially supported by the National Natural Science Foundation of China under the project No. 51604205 and Natural Science Foundation of Hubei Province (No. 2016CFB268). The supports from Fundamental Research Funds for the Central Universities (WUT: 2016IVA046 and 2017IVB018) and the undergraduate research foundation for independent innovation from Wuhan University of Technology (No. 2017-ZH-A1-03 and 2017-ZH-A1-18) are also gratefully acknowledged.

Author Contributions: Yubiao Li designed the experiment and wrote the manuscript while Wanqing Li run the experiment and collected all the data. Qing Xiao involved in the discussion of the results and approved reading the manuscript. Nan He and Zijie Ren analysed data. Clement Lartey and Andrea R. Gerson reviewed and edited the manuscript.

Conflicts of Interest: The authors declare no conflict of interest.

References

1. Córdoba, E.M.; Muñoz, J.A.; Blázquez, M.L.; González, F.; Ballester, A. Leaching of chalcopyrite with ferric ion. Part I: General aspects. *Hydrometallurgy* **2008**, *93*, 81–87. [[CrossRef](#)]
2. Li, Y.; Kawashima, N.; Li, J.; Chandra, A.P.; Gerson, A.R. A review of the structure, and fundamental mechanisms and kinetics of the leaching of chalcopyrite. *Adv. Colloid Interface Sci.* **2013**, *197–198*, 1–32. [[CrossRef](#)] [[PubMed](#)]
3. Hirajima, T.; Suyantara, G.P.W.; Ichikawa, O.; Elmahdy, A.M.; Miki, H.; Sasaki, K. Effect of Mg²⁺ and Ca²⁺ as divalent seawater cations on the floatability of molybdenite and chalcopyrite. *Miner. Eng.* **2016**, *96–97*, 83–93. [[CrossRef](#)]
4. Fuerstenau, M.; Jameson, G.; Yoon, R.H. *Froth Flotation a Century of Innovation*; SME: Littleton, CO, USA, 2007.
5. Bulatovic, S.M. *Handbook of Flotation Reagents Chemistry, Theory and Practice: Flotation of Sulfide Ores*; Elsevier Science: Burlington, VT, USA, 2007.
6. Wang, B.; Peng, Y. The effect of saline water on mineral flotation—A critical review. *Miner. Eng.* **2014**, *66–68*, 13–24. [[CrossRef](#)]
7. Castro, S.; Laskowski, J. Froth flotation in saline water. *KONA Power Part. J.* **2011**, *29*, 4–15. [[CrossRef](#)]
8. Farrokhpay, S.; Zanin, M. An investigation into the effect of water quality on froth stability. *Adv. Powder Technol.* **2012**, *23*, 493–497. [[CrossRef](#)]
9. Moreno, P.; Aral, H.; Cuevas, J.; Monardes, A.; Adaro, M.; Norgate, T.; Bruckard, W. The use of seawater as process water at Las luces copper–molybdenum beneficiation plant in Taltal (Chile). *Miner. Eng.* **2011**, *24*, 852–858. [[CrossRef](#)]
10. Crastró, S. Challenges in flotation of Cu-Mo sulfide ores in sea water. In *Water in Mineral Processing: Proceedings of the First International Symposium*; Drelich, J., Ed.; Society for Mining, Metallurgy, and Exploration: Seattle, WA, USA, 2012.
11. Hancer, M.; Celik, M.S.; Miller, J.D. The significance of interfacial water structure in soluble salt flotation systems. *J. Colloid Interface Sci.* **2001**, *235*, 150–161. [[CrossRef](#)] [[PubMed](#)]
12. Cao, Q.; Wang, X.; Miller, J.D.; Cheng, F.; Jiao, Y. Bubble attachment time and FTIR analysis of water structure in the flotation of sylvite, bischofite and carnallite. *Miner. Eng.* **2011**, *24*, 108–114. [[CrossRef](#)]
13. Parsons, D.F.; Boström, M.; Maceina, T.J.; Salis, A.; Ninham, B.W. Why direct or reversed Hofmeister series interplay of hydration, non-electrostatic potentials, and ion size. *Langmuir* **2009**, *26*, 3323–3328. [[CrossRef](#)] [[PubMed](#)]

14. Weissenborn, P.K.; Pugh, R.J. Surface tension of aqueous solutions of electrolytes: Relationship with ion hydration, oxygen solubility, and bubble coalescence. *Colloid Interface Sci.* **1996**, *184*, 550–563. [[CrossRef](#)]
15. Klassen, V.I.; Mokrousov, V.A. *An Introduction to the Theory of Flotation*, 2nd ed.; Butterworths: London, UK, 1963.
16. Mancera, R.L. Computer simulation of the effect of salt on the hydrophobic effect. *Chemistry* **1998**, *94*, 3549–3559. [[CrossRef](#)]
17. Medrzycka, K.B.; Zwierzykowski, W. The effect of the nature of inorganic ions on hydrocarbon flotation. *Sep. Sci. Technol.* **1988**, *23*, 719–729. [[CrossRef](#)]
18. Henry, C.L.; Craig, V.S.J. The link between ion specific bubble coalescence and Hofmeister effects is the partitioning of ions within the interface. *Langmuir* **2010**, *26*, 6478–6483. [[CrossRef](#)] [[PubMed](#)]
19. Castro, S.; Miranda, C.; Toledo, P.; Laskowski, J.S. Effect of frothers on bubble coalescence and foaming in electrolyte solutions and seawater. *Int. J. Miner. Process.* **2013**, *124*, 8–14. [[CrossRef](#)]
20. Farrokhpay, S. The significance of froth stability in mineral flotation—A review. *Adv. Colloid Interface Sci.* **2011**, *166*, 1–7. [[CrossRef](#)] [[PubMed](#)]
21. Corin, K.C.; Reddy, A.; Miyen, L.; Wiese, J.G.; Harris, P.J. The effect of ionic strength of plant water on valuable mineral and gangue recovery in a platinum bearing ore from the Merensky reef. *Miner. Eng.* **2011**, *24*, 131–137. [[CrossRef](#)]
22. Ramos, O.; Castro, S.; Laskowski, J.S. Copper–molybdenum ores flotation in sea water: Floatability and frothability. *Miner. Eng.* **2013**, *53*, 108–112. [[CrossRef](#)]
23. Laskowski, J.S.; Castro, S.; Ramos, O. Effect of seawater main components on frothability in the flotation of Cu-Mo sulfide ore. *Physicochem. Probl. Miner. Process.* **2013**, *50*, 17–29.
24. Quinn, J.J.; Sovechles, J.M.; Finch, J.A.; Waters, K.E. Critical coalescence concentration of inorganic salt solutions. *Miner. Eng.* **2014**, *58*, 1–6. [[CrossRef](#)]
25. Quinn, J.J.; Kracht, W.; Gomez, C.O.; Gagnon, C.; Finch, J.A. Comparing the effect of salts and frother (MIBC) on gas dispersion and froth properties. *Miner. Eng.* **2007**, *20*, 1296–1302. [[CrossRef](#)]
26. Wang, Y.; Peng, Y.; Nicholson, T.; Lautern, R.A. The role of cations in copper flotation in the presence of bentonite. *Miner. Eng.* **2016**, *96–97*, 108–112. [[CrossRef](#)]
27. Suyantara, G.P.W.; Hirajima, T.; Elmahdy, A.M.; Miki, H.; Sasaki, K. Effect of kerosene emulsion in MgCl₂ solution on the kinetics of bubble interactions with molybdenite and chalcopyrite. *Colloids Surf. A Physicochem. Eng. Asp.* **2016**, *501*, 98–113. [[CrossRef](#)]
28. Craig, V.S.J. Bubble coalescence and specific-ion effects. *Curr. Opin. Colloid Interface Sci.* **2004**, *9*, 178–184. [[CrossRef](#)]
29. Jeldres, R.I.; Arancibia-Bravo, M.P.; Reyes, A.; Aguirre, C.E.; Cortes, L.; Cisternas, L.A. The impact of seawater with calcium and magnesium removal for the flotation of copper-molybdenum sulphide ores. *Miner. Eng.* **2017**, *109*, 10–13. [[CrossRef](#)]
30. Aral, H.; Mead, S.; Cuevas, J.; Davey, K.; Bruckard, W. Desperate times call for desperate measures—The use of seawater in mining and mineral processing. In Proceedings of the AusIMM Sustainable Mining Conference, Kalgoorlie, Australia, 17–19 August 2010.
31. Shirley, D.A. High-resolution X-ray photoemission spectrum of the valence bands of gold. *Phys. Rev. B* **1972**, *5*, 4709–4714. [[CrossRef](#)]
32. Metson, J.B. Charge compensation and binding energy referencing in XPS analysis. *Surf. Interface Anal.* **1999**, *27*, 1069–1072. [[CrossRef](#)]
33. Nagaraj, D.R.; Farinato, R. Chemical factor effects in saline and hypersaline waters in the flotation of Cu and Cu-Mo ores. In Proceedings of the Processing Congress Presented at the XXVII International Mineral, Santiago, Chile, 20–24 October 2014.
34. Blake, T.D.; Kitchener, J.A. Stability of aqueous films on hydrophobic methylated silica. *J. Chem. Soc.* **1972**, *68*, 1435–1442. [[CrossRef](#)]
35. Laskowski, J.S. Coal flotation in solution with a raised concentration of inorganic salts. *Colliery Guard.* **1965**, *211*, 361–366.
36. Li, C.; Somasundaran, P. Reversal of bubble charge in multivalent inorganic salt solutions—Effect of aluminum. *J. Colloid Interface Sci.* **1992**, *148*, 587–591. [[CrossRef](#)]

